# Wear Characteristics of Chilled Aluminum Alloy Reinforced With Nano $ZrO_2$ Metal Matrix Composites (NMMCs) for Automotive Applications

G.. Balakumar[1]
[1]Mechanical Engineering Department, Sir M Visvesvaraya Institute of Technology
Bangalore, Affiliated to Visvesvaraya Technological University
Karnataka, India
g.balakumar72@gmail.com

Joel Hemanth[2]
[2]HMS Institute of Technology,Tumkur
Affiliated to Visvesvaraya Technological
University
Karnataka, India
joelhemanth@hotmail.hotmail.com

***ABSTRACT:*** *This paper aims at development of aluminum alloy (LM 13) reinforced with varying wt.% (3 to 15wt.% in steps of 3) of nano-ZrO2 particles(mesh size 70-90nm) cast using chilling technique which remains an attractive choice among all the solidification processing routes due to its capability of bringing together the advantages of both stir casting and directional solidification. The developed NMMCs and the as cast matrix alloy were hot extruded in a hydraulic press at 250oC. Investigations of microstructural characterization reveal uniform distribution of reinforcement with interfacial integrity between matrix and the reinforcement. Dry sliding wear behavior of the developed NMMCs and matrix alloy was investigated using pin-on-disc apparatus under varying loads. The results exhibit a limiting load known as transitional load beyond which the material (whether matrix alloy or NMMCs) experiences 'seizure'. The transitional load of the developed NMMCs was much higher than matrix alloy. It was also observed that the specific wear rate significantly decreased with increase in reinforcement content but remarkably increases with increase in applied load and sliding distance. However the coefficient of friction registered decreasing trend with increase in sliding distance and reinforcement additions. SEM photograph of worn surfaces of developed NMMCs and matrix alloy reveal delamination of MML (mechanically mixed layer) attributing for seizure.*

**Keywords:** NMMCs, Microstructures, Specific Wear rate, Coefficient of friction, Seizure

**Received:** 24 May 2016, Revised 2 July 2016, Accepted 7 July 2016



## 1. Introduction

As the technology in automotive sectors advances, demand for new materials with ultrahigh mechanical properties and reduced weight capabilities to meet the economics of transportation is highly focused. More recent investigations reveal reinforcing

nano-sized particles in aluminum matrix significantly enhances mechanical properties with retention of ductility [1-2]. Reinforcing hard nano-ceramic particulates in the aluminum alloy emerge superior candidate material for wear resistances, particularly applicable to the components of internal combustion engines such as pistons, cylinder block, connecting rods cylinder liners etc. Aluminum alloys based composites that freeze over a range of temperature experience difficulty in feeding as the solidification progress [3, 4]. Porosity results in pasty type of solidification which commonly occurs in long range freezing alloys, that can be effectively treated by judicious implementation of chills. The chill extracts heat at much faster rate and helps in promoting direction solidification resulting in production of sound castings. Chills are extensively used in foundries for the production of quality castings [5-9].

Open literature search reveal several investigations associated with influence of chills on the solidification and soundness of long freezing range alloy castings [10-14]. The analysis related to dry sliding wear behavior of NMMCs synthesized under the influence of non-metallic chill has been undertaken because from the examination of literature that no data available on silicon carbide chilled Nano-$ZrO_2$ reinforced composite (NMMCs) coupled with hot extrusion. Hence present investigation was undertaken to fill this void.

### 1.1 Volumetric Heat Capacity (VHC) of Chill

The volumetric heat capacity of the chill is evaluated using the relation: $VHC = V \times C_p \times \rho$ as shown in the Table 1. Where V, Cp& ρ are the volume, specific heat & density of the chill material respectively.

## 2. Experimental procedure

### 2.1 Material preparation

In this research work, nano-sized $ZrO_2$ particulates were incorporated into aluminum alloy (standard (LM 13) fabricated via chilling technique followed by hot extrusion. The chemical composition of the matrix alloy and the properties of the reinforcement are shown in the Table 1 & 2 respectively. The size of the nano-$ZrO_2$ particulates dispersed varies from 70 to 90 nm. The amount of reinforcement addition varied from 3 to 15 wt. % in steps of 3. The primary processes include heating of Al alloy in a graphite crucible up to 650$^o$C to which the preheated reinforcement (heated up to 650$^o$ C) was added and stirred well by a mechanical impeller. The impeller speed was maintained at 400 rpm to generate vortex in order to get uniform distribution of the reinforcement in the liquid melt. The reinforcement treated mixture was poured into a dry sand mold containing silicon carbide as end chill to produce plate type of casting following AFS mould of size 225mm X 150mm X 25mm prepared using silica sand with 5% bentonite as binder and 5% moisture and dried using air blower. In secondary processing, the developed NMMCs and the as cast matrix alloy were hot extruded in a hydraulic press at 250$^o$C, to about 2mm (thickness reduced from 25mm to 23m).

### 2.2 Microstructure preparation

The samples for microstructural characterization were cut near to the chill end of final cast components. Samples were prepared following standard metallographic procedure and are itched using kellers reagent.

### 2.3 Dry sliding wear tests

The Dry sliding wear tests was performed using standard computerized pin on disc (POD) friction and wear monitoring test rig (Ducom make India). The specimens prepared (chosen near to chill end) were of 6mm diameter and 40mm length. Varying loads of 10N, 20N, 40N & 50N were applied at constant disc rotational speed of 600 rpm against EN 31 steel(hardness-HRC 60) with track radius maintained at 90mm. The surface of the samples was ground with emery paper for providing effective contact with the steel disc.

## 3. Results

### 3.1. Microstructural Analysis

Microstructural observations confirmed that the structure of chilled matrix alloy is finer than that of un-chilled matrix alloy (refer Fig. 1 & 2). Microstructural observation of developed NMMCs reveal uniform distribution of reinforcement, good reinforcement matrix interfacial integrity with significant grain refinement (refer Figure 3,4 & 5 (a)&(b).This is due to the judicious implementation of parameters such as effective stirring rate, good wetting achieved through pre-heat treatment of reinforcement and effective chilling. As solidification progress, semi-solid (pasty mass) coexists with the fully solid and fully liquid zones containing nano-$ZrO_2$ particles. The freezing shrinkage of the molten metal is compensated by flow of pasty mixture of solid and liquid. Hence freezing shrinkage and the volume shrinkage due to the solid contraction on the dendrites must be compensated by the flow of

liquid metal on the interdendritic channels ensuring perfect bond between the reinforcement and the matrix. Establishing steep temperature and solidification gradient during solidification process by employing chills will ensure proper feeding of metal to the regions of last solidifying liquid; minimize shrinkage porosity and enhancing good reinforcement matrix bond.

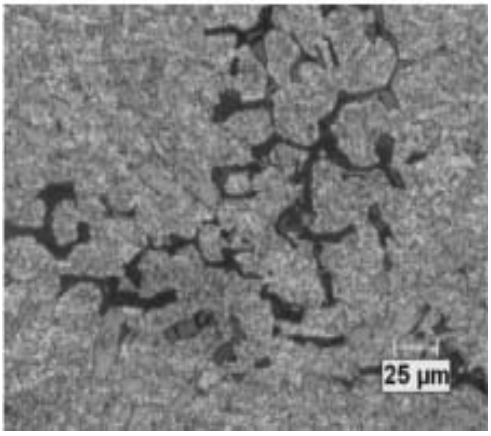


Figure 1. Optical microstructure of un-chilled matrix alloy (at 200 X)

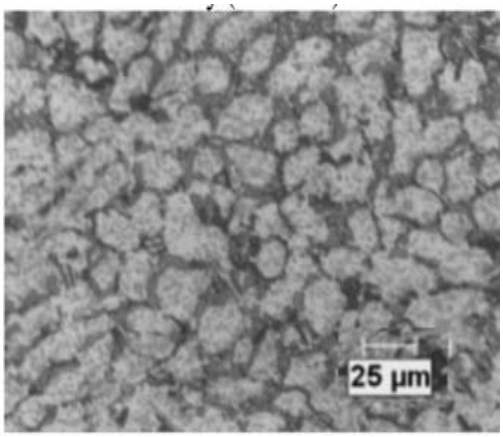


Figure 2. Optical microstructure of chilled matrix alloy (at 200 X)

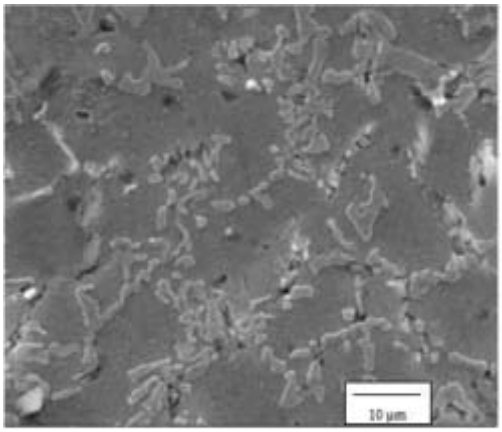


Figure 3. SEM micrograph of NMMCs with 6 Wt.% $ZrO_2$ at 2000 X

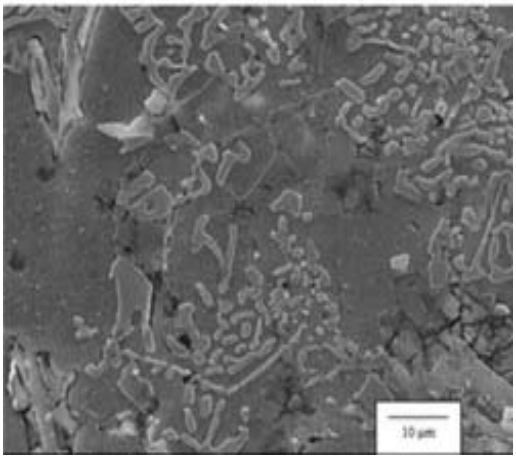


Figure 4. SEM micrograph of NMMCs with 9 Wt.% $ZrO_2$ at 2000 X

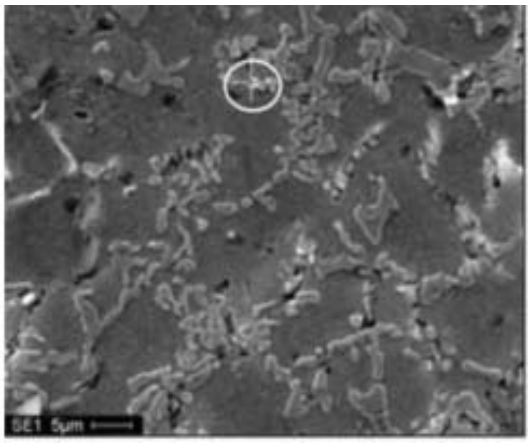


Figure 5(a). SEM micrograph of NMMCs with 12 Wt.% $ZrO_2$ at 2000 X

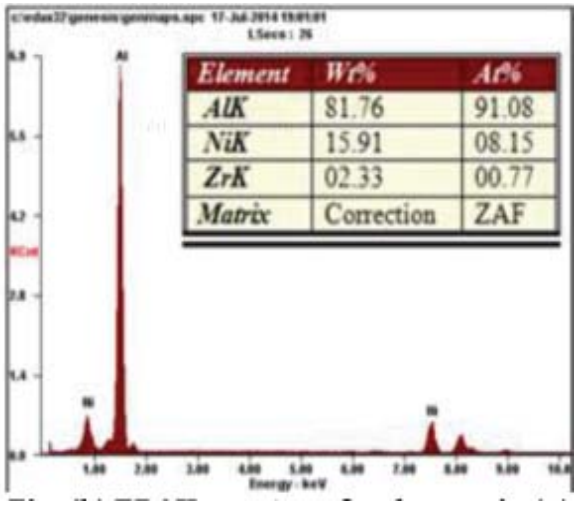


Figure 5(b). EDAX spectra of red cross in (a)

### 3.2.1 Effect of applied load on specific wear rate

The specific wear rates of the matrix alloy and the developed NMMCs containing varying wt % of reinforcement were ploted against varying loads of 10N, 30N, 40N & 50N are as shown in the Figure6&7(a) to (d) respectively. It obseved from results that, the specific wear rate increases with applied load considerably before reaching transition (mild to seviere) and beyond transition, the specific wear rate increases drastically with increase in load. Sudden increase in specific wear rate at perticular load can be termed as 'seizure load'. Also, observed that the specific wear rate lenearly increases with increase in applied load up to 30 N for both matrix alloy and NMMCs (refer Figure 7. ). However, the specific wear rate of the matrix alloy is higher than that of nanocomposites. The specific wear rate of the matrix alloy for the applied load of 10 N is 5.3e-5mm$^3$/Nm and found to increased to 5.50e-5 mm$^3$/Nm at the applied load of 30N, during the course, the specific wear rate of matrix alloy exhibits a lenear trend. Beyond the applied load of 30 N, the matrix alloy tends towards getting seized and exhibits sevier specific wear rate as high as 9.91e-5 mm$^3$/Nm at the applied load of 50 N. The NMMC containing 9 wt.% $ZrO_2$ registers a specific wear rate in the order 2.59e-5 mm$^3$/Nm to 3.36e-5mm$^3$/Nm with the applied load ranging from 10 N to 30 N and beyond this load, the NMMC (9 wt.% $ZrO_2$) registered specific wear as high as 5.12e-5mm$^3$/Nm at 50 N of applied load.It is very intresting to note that irrrespective of the material (alloy or nanocomposites) beyond the transitinal load, the materials experiences 'seizer'. The transition load for the matrix alloy almost starts beyond 30 N of applied load where as for NMMC the transitional load starts beyond 40N (refer Fig 7). In the case of developed NMMCs, significant increase in the transition load can be attributed to the presence and uniformly distributed hard ceramic nano-sized $ZrO_2$ particulates in the matrix material.

### 3.2.2 wear rate

The specific wear rate as a function of sliding distance for the matrix alloy and the developed NMMCs with varying loads from of 10 to 50 N are as shown in the Figure 8 (a) to (d). It is obsorbed that the specific wear rate of matrix alloy follows lenear trend for a initial slididing distance up to 1500 m and beyond 1500 m the trend changes and exhibits significant increase in specific wear rate. The specific wear rate of the NMMCs is almost constant with the sliding distance and detoriates with increase in reinforcement content in the matrix. The matrix alloy undergoes sevier specific wear rate beyond 1500 m of sliding distance migrating toward seizure with the applied load beyond 30N. However the NMMCs maintains almost a lenear trend with the sliding distance up to 2000m with the applied load of 10 N. Similar trend is noticed for all the samples of NMMCs even with applied loads of 30 N to 50N.

### 3.2.3 Effect of sliding distance on coefficient of Friction

The plots of coefficient of friction as a function of sliding distance with varying applied loads for the samples of developed NMMCs and the matrix alloy are as shown in the Figure9 (a) to (d). It is noticed that the frictional coefficients of both matrix alloy and developed NMMCs registered a detoriated trend with increase in sliding distance.The coefficient of friction for NMMCs is significantly lower than that of matrix alloy and it is intresting to note that the coefficient of friction decreases with addition of nano-$ZrO_2$ particle.This reduce in the frictional coefficients can be primarily attributed to due to addition and uniform distribution of reinforcement (nano-$ZrO_2$ particles) on the specimen surface but there is no definite trend for comparsion of coefficient of friction between matrix alloy and the NMMCs[16]. It is also observed that the coefficient of friction of the matrix alloy and the NMMCs varies up and down within a narrow range against sliding distance and in case of NMMCs containing 9wt.% of $ZrO_2$, the coefficient of friction varies between 0.20 to 0.24 against the sliding distance up to 2000 m.

### 3.3 Worn surface analysis

Worn surface of matrix alloy and developed NMMCs at various applied loads are as shown in the Fig. 9(a) to (g). The worn surface of matrix alloy at 10 N of applied load reveal formation of parallel and longitudinal grooves in series (referFig. 9(a)). In case matrix alloy experiencing seizure at 50 N load, type of wear was charecterized by material flow in the direction of sliding, formation of cavities at the cost of delamination and material tearing from the surface as shown in the Fig. 9(b). Wear debris, smoother MML formation and damaged MML were associated with NMMCs containing 3wt. % of $ZrO_2$ worn at the applied load of 30 N as shown the Fig. 9(c) & (d). In the case of NMMCs reinforced with 6 wt.% of $ZrO_2$ migrating towards seizure from the transition load as shown in the Fig. 9(e) & (f), in which formation and delamination MML resulting in formation of cavities, and tearing of material. Surface cracks and localized adhersion between specimen surface and counter surface as shown in the Fig. 9(g) that has occurred at higher loads with the NMMCs containing 12 wt. % of $ZrO_2$.

## 4. Conclusions

Chilling technique coupled with hot extrusion applied for the development of NMMCs reveal fine grain refinement, fairly uniform distribution of reinforcement (vortex route). Specific wear rate significantly decreases with increase weight percentage

| Chill material | Density g/cc | Specific heat J/Kg K | Thermal conductivity W/mK | VHC for 35mmchill thick |
|---|---|---|---|---|
| Silicon carbide | 2.36 | 1.095 | 0.031 | 538.15 |

Table 1. Volumetric heat capacity of silicon carbide Chill

| Elements | Zn | Mg | Si | Ni | Fe | Mn | Al |
|---|---|---|---|---|---|---|---|
| Wt.% | 0.5 | 1.4 | 12 | 1.5 | 1.0 | 0.5 | Bal |

Table 2. Chemical composition of matrix alloy (LM 13)

| Elements | Density gm/cm3 | Melting point C° | UTS Mpa | VHN | Young's modulus GPa | Supplier |
|---|---|---|---|---|---|---|
| $ZrO_2$ | 8.1 | 1860 | 425 | 150 | 98 | Nano Structured & Amorphous Material, Inc.,USA |

Table 3. Properties of reinforcement

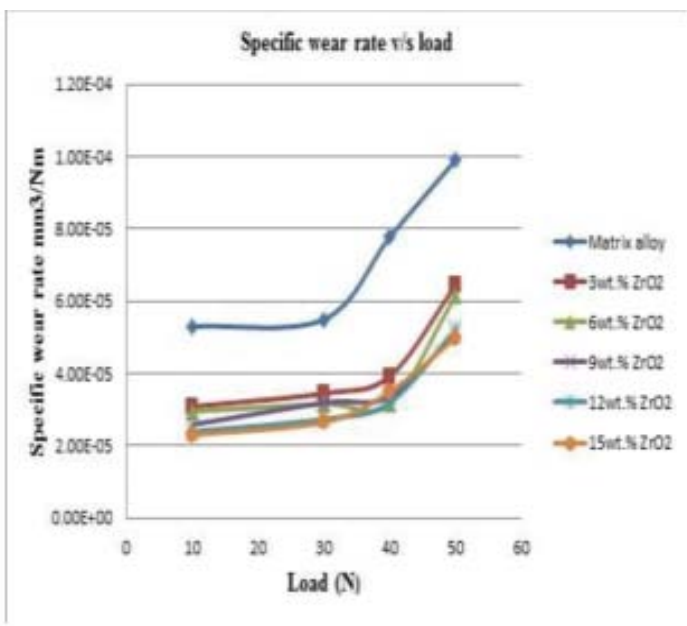


Figure 6. Specific wear rate v/s load

of reinforcement addition in the matrix alloy but increases significantly as applied load and sliding distance increases. The coefficient of friction of both matrix alloy and NMMCs registered a deteriorating trend with increase in sliding distance & reinforcement additions. The coefficient of friction for NMMCs is significantly lower than that of matrix alloy and varies up and

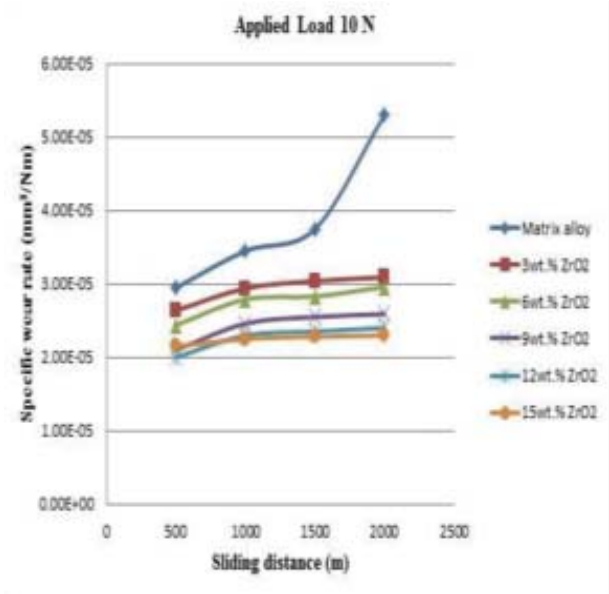


Figure 7(a). Specific wear rate v/s sliding distance

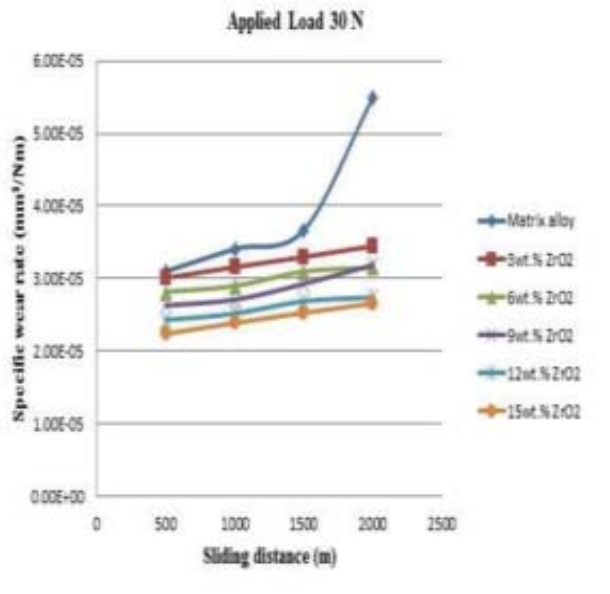


Figure 7(b). Specific wear rate v/s sliding distance

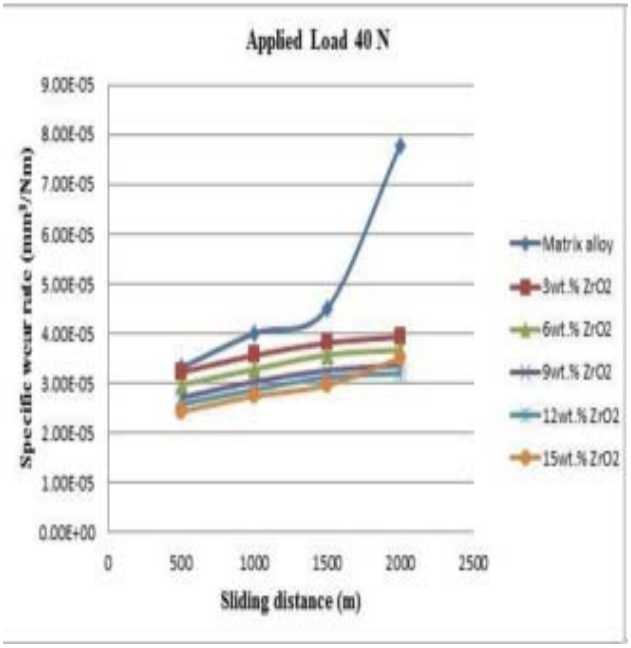


Figure 7(c). Specific wear rate v/s sliding distance

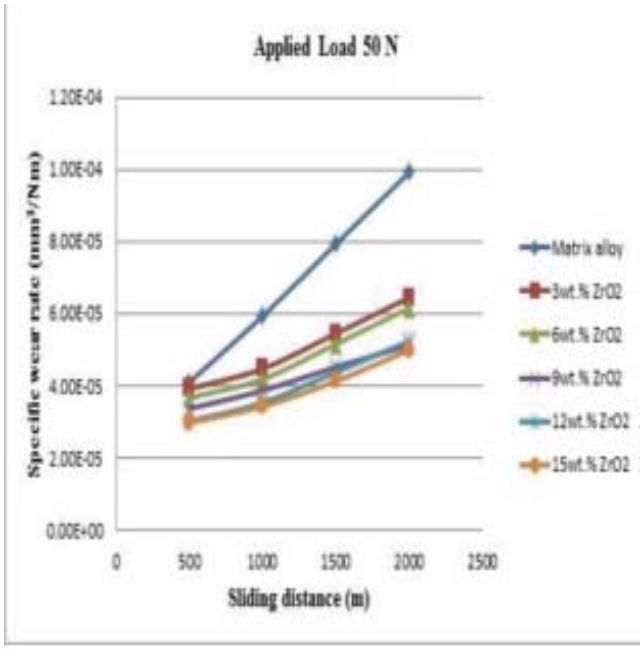


Figure 7(d). Specific wear rate v/s sliding distance

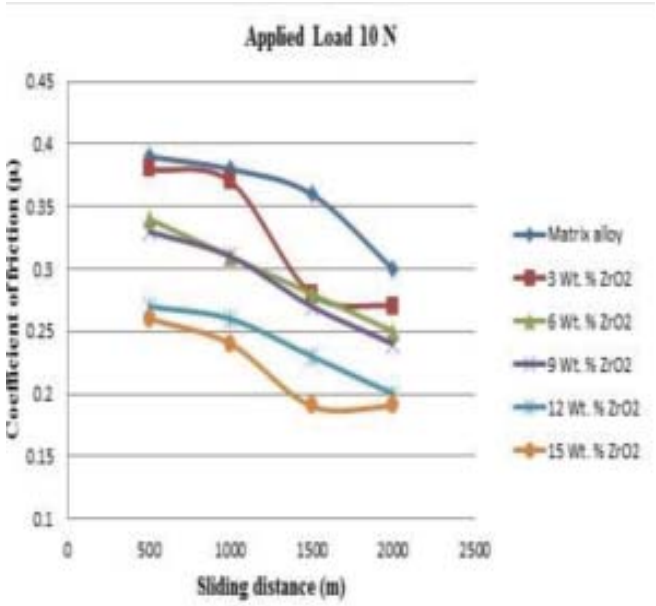


Figure 8(a). Coefficient of friction v/s sliding distance

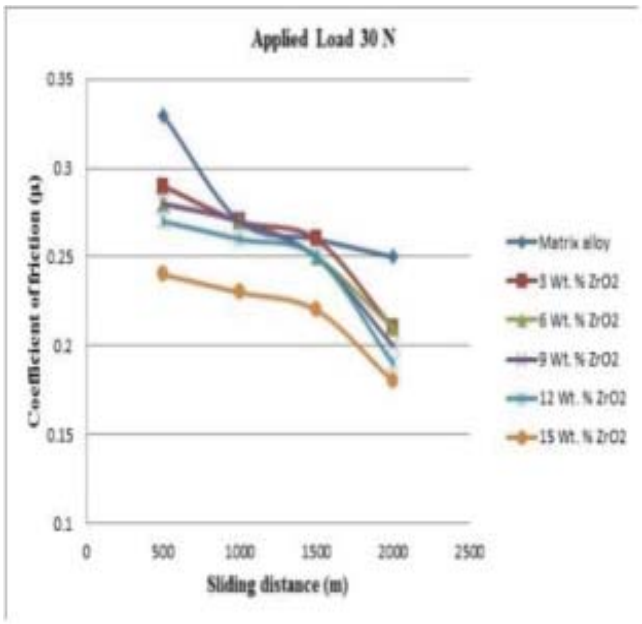


Figure 8(b). Coefficient of friction v/s sliding distance

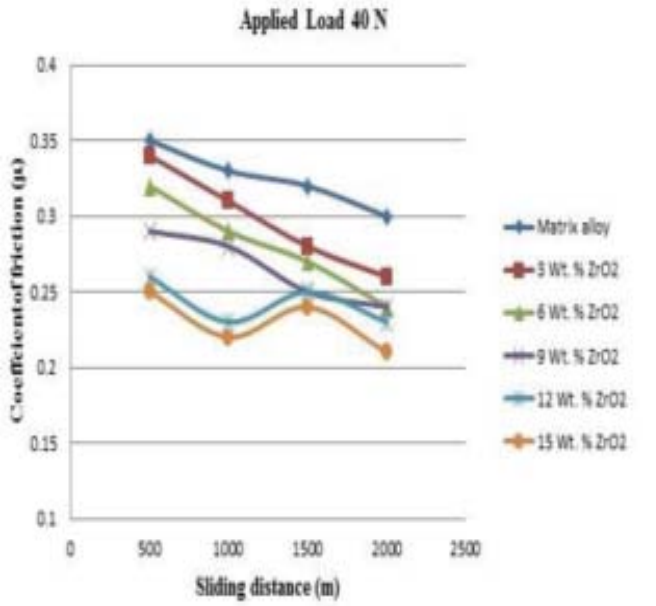


Figure 8(c). Coefficient of friction v/s sliding distance

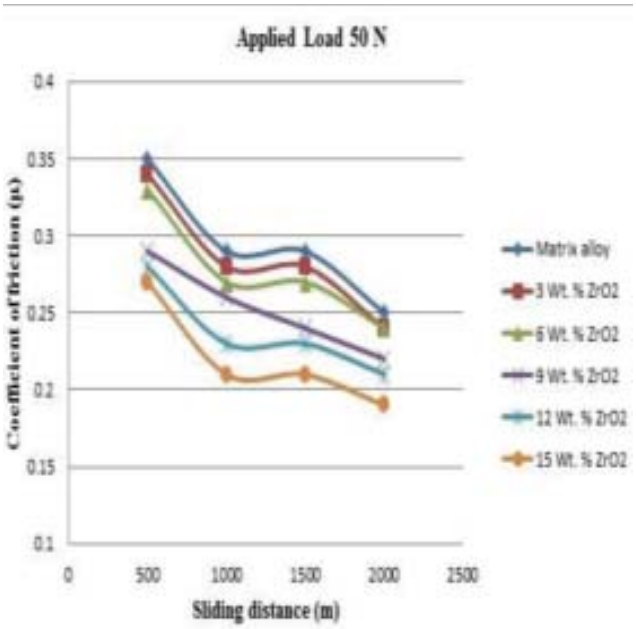


Figure 8(d). Coefficient of friction v/s sliding distance

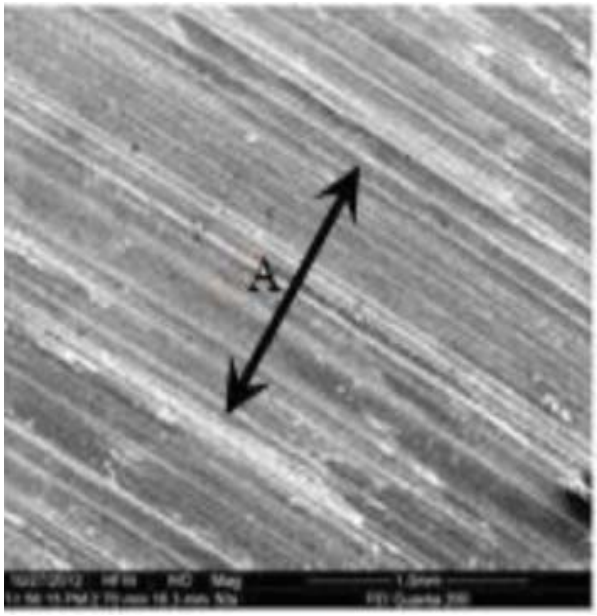


Figure 9(a). SEM micrograph of matrix alloy reveal parallel & longitudinal grooves (A) worn at 10N (at 500 X, 100 µm)

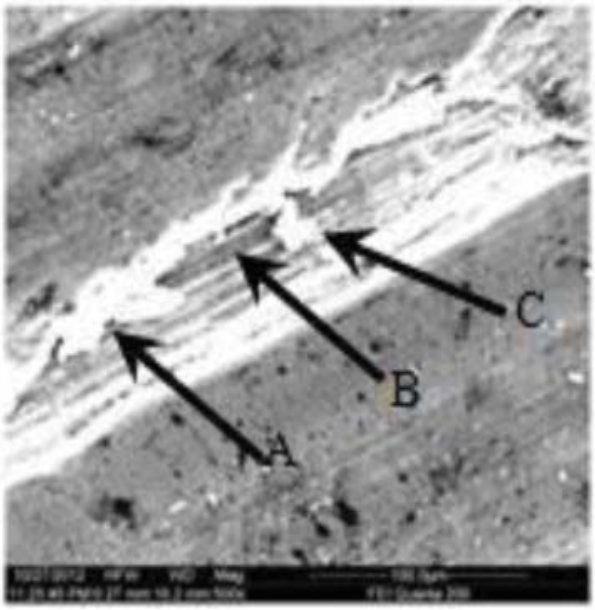


Figure 9(b). SEM micrograph of matrix alloy worn at 50N reveal delamination ML (A) cavities (B) tearing of material (C), (at 500 X, 100 µm)

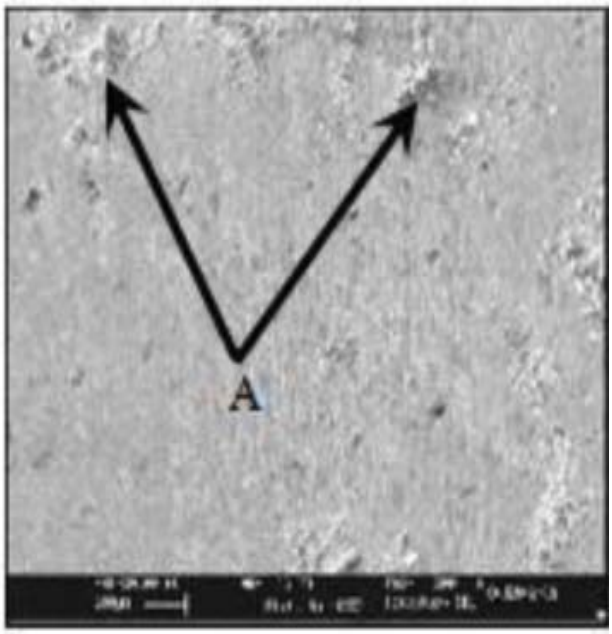


Figure 9(c). SEM micrograph of worn NMMC(3wt.% $ZrO_2$) at 30N reveal wear debris (A), (at 500 X, 100 µm)

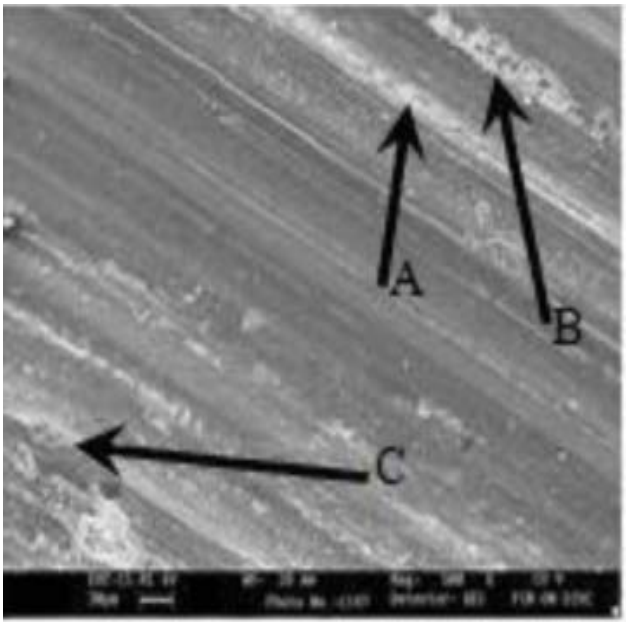


Figure 9(d). SEM micrograph of NMMC( 3wt. % $ZrO_2$) worn at 40N reveal smoother MML (A) & damaged MML(B & C), (at 500 X, 100 mm)


Figure 9(e). SEM micrograph of NMMC (6Wt. % $ZrO_2$) worn at 40N revealsmoothen MML (A) &damageregion (B), AT (500 X, 100 µm)


Figure 9(f). SEM micrograph of NMMC ( 6Wt. % $ZrO_2$) worn at 50N delamination of MML(A & B) formation of cavities (C), AT (500 X, 100 µm)

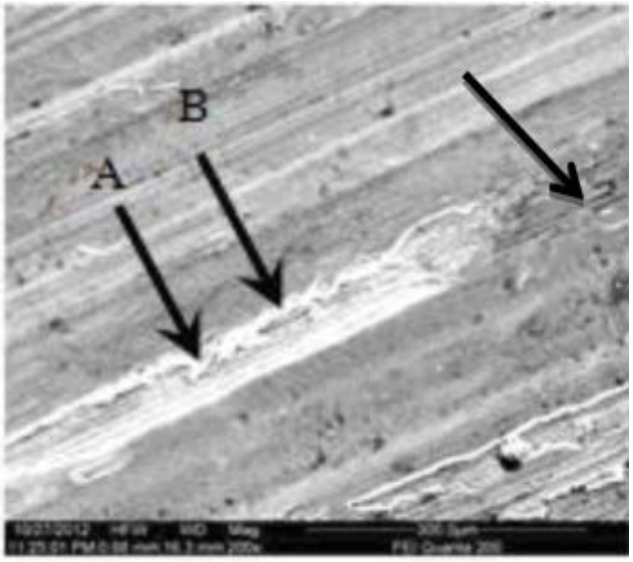


Figure 9(g). SEM micrograph of NMMC(12Wt. % $ZrO_2$) worn at 50N reveal local adhesion (A & B) and surface cracks (C), AT (500 X, 100 µm)

down within a narrow range. The transitionlimiting load for matrix alloy is 30 N beyound which the matrix material undergoes seizure where as in the case of developed NMMCs, the transitionlimiting load has enhanced to 40 N. The factors identified for the specimens experiencing seizures are due to delamination of MML and formation of cavities at the cost of delamination.

**References**


[1] Mazahery, A., Abdizadeh, H., Baharvandi, H R. (2009).Development of high-performance A356/nano-Al2O composites. *J. Mater SciEngg* A, 2009, 518 61-64.

[2] Habibnejad, Korayema M., Mahmudia R, Pooleb, W. J. (2009). Enhanced properties of Mg-based nano-composites reinforced with Al2O3, nano-particles. *J. Mater SciEngg A*, 519 (1-2) 198-203.

[3] Reddy, G.P., Br, P.K.(1976). Foundaryman 69. 265.

[4] Cambell, X. (1991). Castings, Butterworth-Heinemann,

[5] Hemanth, Joel., Seah, KWH, Sharma, S C. (1996). Wear characteristics of sub zero chilled cast iron. *Wear* 192: 125-34.

[6] Hemanth, Joel (2005). Effect of microstructure on mechanical behavior of chilled Pb-Sb-Sn-As alloy-Al2SiO5 MMCs . *J. Microstruct Mater Proper ;* 1:65-74

[7] Hemanth, Joel.(1998). Effect of cooling rate on the dendrite arm spacing and ultimate tensile strength of cast iron. *Mater Sci* 33. 17-23.

[8] Hemanth, Joel. (2006). Development, mechanical properties and fracture toughness of chilled Pb/Sb/Sn/As alloy-Al2 SiO5 (Kaolinite) MMCs. *J Compos Mater* 40:538-47.

[9] Flinn, RA, (1959). Action of chills on soundness of Al-4.5%Cu alloy casting. *Trans AFS* 67. 377-85.

[10] Couture, A. (1966).Non-equilibrium phase distribution in A-Si alloys. *Trans AFS* 74. 155-64.

[11] Chamberlin, M.V., Mezoff, J.G. (1946). Effect of chilling on strength and hardness of Al-Cu alloy plate castings. Trans AFS 54. 648-654.

[12] Seshan, S., Murthy KSS(1968). Application of chills for aluminum-magnesium alloy castings. Br Foundryman 1968;61:330-9.

[13] Berry, J.T. (1970). Solidification behavior of Al-12Si end chilled plate casting on dendrite arm spacing and microstructure. Trans AFS 78:410-21.

[14] Prabhakar, KV., Sheshadri, MR. (1997). Influence of chills on soundness of Al-12%Si alloy castings. *Trans AFS* 1997;87:368-77.

[15] Hemanth, Joel (2000). Action of chill on soundness and ultimate tensile strength of aluminum-quartz particulate composite,*J. Alloys and Compds.* 296. 193-200.

[16] Hassan, S.F., Gupta, M (2006). Effect of different types of nano-size oxide particulates on microstructure and mechanical properties of elemental *Mg, J. Mater. Sci***.** 41 (2006) 2229-2236.